Superlattices and Microstructures, Vol. 12, No. 1, 1992

THE THICKNESS DEPENDENCE OF THE BAND GAP OF α-Sn FILMS

B.I.Craig
Surveillance Research Laboratory
Defence Science and Technology Organisation
P.O.Box 1500, Salisbury, SA 5108, Australia

(Received 31 March 1992)

A theoretical treatment of the electronic structure of thin α-Sn films is presented. The energy levels describing the electron sub-bands are calculated for (100) and (111) oriented films. The symmetry induced zero band gap obtained for the bulk solid is found to open for a thin film to form a gap between the valence sub-band manifold and the conduction sub-band manifold.

1 Introduction

α-Sn is a zero band gap semiconductor with degenerate valence and conduction bands at the centre of the Brillouin zone (k=0). In films of finite thickness the electron motion in the direction normal to the film surface ($|k_z|>0$) is quantised into discrete sub-bands and an energy gap between the valence and conduction band manifolds may possibly occur. The deposition of such material onto suitable substrates may lead to possible band gap engineering of α-Sn quantum well structures. Theoretical examinations of such films have been limited so far either by approximations [1] or by restriction to a very small number of layers [2] and have not fully explored the electronic structure induced by the quantum size effect. On the other hand there has been considerable experimental interest [3-9] given to these films. This work has examined the band gap properties [3,4], the quantum confinement of carriers [8] and the electronic structure induced by the interface with the substrate [9].

In this paper the earlier theoretical treatment [1] has been greatly expanded to obtain a description of the electronic structure of both (100) and (111) α-Sn films. In the earlier work the spin orbit interaction and the dispersions of the sub-bands through the two dimensional Brillouin zone were not adequately included. That method only treated the valence band minima and maxima at k=0. In this paper the spin orbit interaction which leads to the zero band gap degeneracy is included into the calculation of all the valence sub-band manifolds and also those conduction sub-band manifolds immediately above the band gap.

2 Theory

The method for modelling the electronic structure of the thin film is an extension of the tight binding method for semiconductors [10-12]. The application of the method to the bulk electronic structure of α-Sn with the additional inclusion of the spin orbit interaction is initially described.

2.1 The Electronic Structure of α-Sn

The bulk electronic structure is modelled by the one-electron Hamiltonian

$$H = H^0 + V_{so} \qquad (1)$$

where

$$H^0 = -\nabla^2 + V(\underset{\sim}{r}) \qquad (2)$$

and the potential $V(\underset{\sim}{r})$ is periodic and V_{so} is the spin orbit interaction term. The potential $V(\underset{\sim}{r})$ is expanded as a plane wave summation with respect to the reciprocal lattice vectors $\{ \underset{\sim}{g} \}$ and the two diamond lattice position vectors are

$$\underset{\sim}{\tau}_1 = -\underset{\sim}{\tau}_2 = \underset{\sim}{\tau}_0 = \tfrac{1}{8}(a,a,a)$$

and a is the lattice constant equal to 6.49 Å, giving

$$V(\underset{\sim}{r}) = \sum_g V(\underset{\sim}{g}) \cos(\underset{\sim}{g}\cdot\underset{\sim}{\tau}_0) \exp(i\underset{\sim}{g}\cdot\underset{\sim}{r}) \qquad (3)$$

The electronic structure can be solved

0749-6036/92/050001 + 06 $08.00/0

where the wave-functions are expanded either in terms of the plane wave basis

$$\psi_n(\mathbf{k},\mathbf{r}) = \sum_g c_n(\mathbf{k}+\mathbf{g}) \exp(i(\mathbf{k}+\mathbf{g})\cdot\mathbf{r}) \qquad (4)$$

or in terms of a localised orbital basis, where

$$\psi_n(\mathbf{k},\mathbf{r}) = \sum_j \sum_{\boldsymbol{\tau}} b_{nj\boldsymbol{\tau}}(\mathbf{k}) \Phi_{jk}(\mathbf{r}-\boldsymbol{\tau}) \qquad (5)$$

and

$$\Phi_{jk}(\mathbf{r}-\boldsymbol{\tau}) = (N_c)^{-1/2} \sum_{\mathbf{R}}^{N_c} \exp(i\mathbf{k}\cdot\mathbf{R})\ \phi_j(\mathbf{r}-\mathbf{R}-\boldsymbol{\tau}) \qquad (6)$$

and $\{\phi_j(\mathbf{r}-\boldsymbol{\tau})\}$ are the set of localised functions sited at $\tau=\tau_1,\tau_2$. The summation in equation 6 is over the N_c unit cells which make up the face centred cubic lattice.

In the current description of the electronic structure of thin films the localised orbital basis is used. However, to examine the suitability of this basis, the electronic structure of the three dimensional bulk solid is calculated with both the plane wave basis and the localised orbital basis. The electronic structure arising from H° for the plane wave basis is straightforwardly obtained from

$$\sum_g [\{ |\mathbf{k}+\mathbf{g}|^2 - E_n(\mathbf{k}) \}\delta_{g',g} + V(\mathbf{g}'-\mathbf{g})\cos((\mathbf{g}'-\mathbf{g})\cdot\boldsymbol{\tau}_0)]c_n(\mathbf{k}+\mathbf{g}) = 0 \qquad (7)$$

and for the localised basis set

$$\sum_j \sum_{\boldsymbol{\tau}} \{ H_{j'\boldsymbol{\tau}',j\boldsymbol{\tau}} - E_n(\mathbf{k}) S_{j'\boldsymbol{\tau}',j\boldsymbol{\tau}} \} b_{nj\boldsymbol{\tau}}(\mathbf{k}) = 0 \qquad (8)$$

which requires greater computation. The overlap S and Hamiltonian H matrix elements are given by

$$S_{j'\boldsymbol{\tau}',j\boldsymbol{\tau}}(\mathbf{k}) = \Omega_{BZ} \sum_g \alpha^*_{j'}(\mathbf{k}+\mathbf{g})\ \alpha_j(\mathbf{k}+\mathbf{g}) \times \exp[i(\mathbf{k}+\mathbf{g})\cdot(\boldsymbol{\tau}'-\boldsymbol{\tau})] \qquad (9)$$

and

$$H^{\circ}_{j'\boldsymbol{\tau}',j\boldsymbol{\tau}}(\mathbf{k}) = \Omega_{BZ} \sum_g \alpha^*_{j'}(\mathbf{k}+\mathbf{g})\ \alpha_j(\mathbf{k}+\mathbf{g}) \times |\mathbf{k}+\mathbf{g}|^2 \exp[i(\mathbf{k}+\mathbf{g})\cdot(\boldsymbol{\tau}'-\boldsymbol{\tau})]$$

$$+ \sum_g \sum_{g'} \alpha^*_{j'}(\mathbf{k}+\mathbf{g}')\alpha_j(\mathbf{k}+\mathbf{g})\cos[(\mathbf{g}'-\mathbf{g})\cdot\boldsymbol{\tau}_0] \times V(\mathbf{g}'-\mathbf{g})\exp(i[(\mathbf{k}+\mathbf{g}')\cdot\boldsymbol{\tau}'-(\mathbf{k}+\mathbf{g})\cdot\boldsymbol{\tau}]) \qquad (10)$$

and $\alpha(q)$ is the Fourier transform of $\phi(r)$, and Ω_{BZ} is the volume of the three dimensional Brillouin zone.

The bandstructure is obtained for both types of basis. The localised orbital basis is chosen to consist of Slater functions of the form

$$\phi_j(\mathbf{r}) = c_j\, r^{n_j} \exp(-\beta_j r)\ Y_{l_j m_j}(\theta,\phi)$$

where there are two s orbitals ($n=1,\beta=1.7$ and $n=2,\beta=1.3$), a single p radial function ($n=2,\beta=1.05$) and a single d radial function ($n=2,\beta=1.0$), giving a total of 10 orbitals for each spin and therefore 20 orbitals on each atomic site.

The potential V(r) is modelled by a local pseudopotential where V(3)=-0.200, V(8)=-0.002, and V(11)=0.040 Rydbergs, which is consistent with other bandstructure calculations [15,16].

The resulting energy levels at the main Brillouin zone symmetry points for H° are shown in table 1 for both basis sets. The plane waves basis consists of 113 functions. The comparison clearly demonstrates the ability of the localised orbital set to reproduce the main features of the dispersions within the valence bands and the low lying conduction bands of the bulk α-Sn electronic structure.

The electronic structure, where the spin orbit term is now included, is straightforwardly obtained by adding terms into the p orbital matrix sub-block as along the lines of other tight binding schemes [13,14]. In the current method the orbitals belong to a non-orthogonal basis. A spin orbit parameter of $\lambda=0.016$ Rydbergs is empirically determined to reproduce the essential features for the valence bands and the low lying conduction bands at the Γ point of the α-Sn bandstructure. This bandstucture is illustrated in figure 1 for the (100) and (111) dispersions, and the energy levels for the main Brillouin zone symmetry points are displayed in table 1.

The results of the non-local pseudopotential calculation with spin orbit interaction [16] are also included in table 1 for comparison. The non-local pseudopotential yields an improved description for the full valence band width. The current work is interested in those energy levels near the band gap and the ease which the method for examining the bulk electronic bandstructure can be extended to treat the thin film. As a result the simpler local pseudopotential is preferred.

This method can be easily extended to binary zincblende systems such as HgTe [17,18]. Other methods such as the nearest neighbour semi-empirical tight binding method [19] also produce good

Table 1

The bandstructure energy levels (eV) at the Brillouin Zone symmetry points of α-Sn. The bandstructures of H^o for both the plane wave (PW) and localised orbital (LCAO) sets, and H^o+V_{sp} for LCAO and that of reference 16 are displayed.

Symmetry Point	Level	Hamiltonian			
		H^o		H^o+V_{so}	
		PW	LCAO	LCAO	NLP
Γ	Γ_6^v	-9.30	-9.27	-9.55	-11.34
	Γ_7^v			-0.81	-0.80
	Γ_8^v	0.00	0.00	0.00	0.00
	Γ_7^c	-0.18	-0.15	-0.42	-0.42
	Γ_6^c			1.64	2.08
	Γ_8^c	2.80	2.92	2.88	2.66
L	L_6^v	-7.91	-7.85	-8.15	-9.44
	L_6^v	-5.44	-5.38	-5.70	-6.60
	L_6^v			-1.37	-1.68
	$L_{4,5}^v$	-0.89	-0.74	-0.95	-1.20
	L_6^c	0.43	0.52	0.15	0.14
	L_6^c			2.97	3.48
	$L_{4,5}^c$	3.53	3.60	3.49	3.77
X	X_5^v	-6.64	-6.54	-6.89	-7.88
	X_5^v	-1.85	-1.81	-2.14	-2.75
	X_5^c	1.10	1.26	0.87	0.90

representations of the bandstructures of these semiconductor materials.

2.2 The Thin Film

In a film of finite thickness L containing N layers, the three dimensional Brillouin zone is replaced by a two dimensional zone (k'_x,k'_y) and

$$k'_z = m\pi/L.$$

describes the mth sub-band of band n. A set of N position vectors $\{\lambda_p\}$ describe the unit cell for the two dimensional bandstructure. Each site λ_p corresponds to the position of an atom in the pth layer. The atoms are assumed to occupy the expected bulk positions. The odd numbered layers are τ_1 sites and the even numbered layers are τ_2 sites for both the (100) and (111) films.

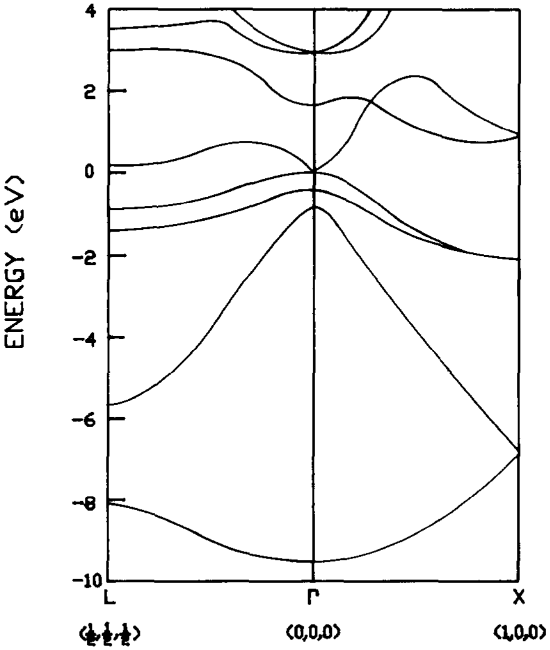

Figure 1: The bulk electronic bandstructure of α-Sn in the (100) and (111) directions.

The Hamiltonian is written as

$$H = T + V + U + V_{so}$$

where V(r) is the periodic potential of the α-Sn and U is the perturbation by the walls of the quantum well.

The orbitals sited within the surface layers will gain the greatest contribution from U(r). The matrix elements <i|U|i> for those orbitals will be positive and describe the barrier confining the valence electrons within the quantum well and will vary with the nature of the barrier material and the atomic reconstruction within the surface α-Sn layer. A simple positive contribution from U , given by

$$\langle i|U|j\rangle = U_o\delta_{ij}$$

is assumed for those orbitals i and j sited on the surface. This simple form provides a basic qualitative model for the barrier. This very approximate treatment describes the increase in potential energy felt by the part of the orbital within the barrier region. In the case of the surface the barrier is several eV high. A range of values for U_o are investigated.

The wavefuction for each sub-band is written as a sum over layer summations

$$\varphi_{nm}(\underset{\sim}{k},\underset{\sim}{r}) = \sum_{\lambda_p}^{N}\sum_{j} C_{nm}(\underset{\sim}{k},\underset{\sim}{\lambda}_p)\ \Phi_j(\underset{\sim}{k},\underset{\sim}{r}-\underset{\sim}{\lambda}_p) \tag{11}$$

where Φ_j is a layer summation over the N_L lattice sites in the pth layer,

$$\Phi_j(\underset{\sim}{k},\underset{\sim}{r}-\underset{\sim}{\lambda}_p) = (N_L)^{-1/2}\sum_{R}^{N_L}\phi_j(\underset{\sim}{r}-\underset{\sim}{R}-\underset{\sim}{\lambda}_p)\exp(i\underset{\sim}{k}\cdot\underset{\sim}{R})$$

and k belongs to the two dimensional Brillouin zone. The overlap S and Hamiltonian H^{o}=T+V matrix elements with respect to the layer summations $\Phi_j(\underset{\sim}{k},\underset{\sim}{r}-\underset{\sim}{\lambda}_p)$ are given by

$$S_{ip,jq}(\underset{\sim}{k}) = S_{ij}(\underset{\sim}{\lambda}_q-\underset{\sim}{\lambda}_p\ ,\underset{\sim}{k})$$

and $$T_{ip,jq}(\underset{\sim}{k}) = T_{ij}(\underset{\sim}{\lambda}_q-\underset{\sim}{\lambda}_p\ ,\underset{\sim}{k})$$

and $$V_{ip,jq}(\underset{\sim}{k}) = V_{ij}^{m}(\underset{\sim}{\lambda}_q-\underset{\sim}{\lambda}_p\ ,\underset{\sim}{k})$$

where m=1 if λ_p is a τ_1 site and similarly m=2 if λ_p is a τ_2 site.

These matrix elements are obtained from the following expressions

$$S_{ij}(\underset{\sim}{\lambda},\underset{\sim}{k}) = \frac{\Omega_{BZ}}{N'}\sum_{q}^{N'}\sum_{g}\alpha_i^*(\underset{\sim}{q}+\underset{\sim}{k}+\underset{\sim}{g})\ \alpha_j(\underset{\sim}{q}+\underset{\sim}{k}+\underset{\sim}{g})\ \exp(-i(\underset{\sim}{q}+\underset{\sim}{k}+\underset{\sim}{g})\cdot\underset{\sim}{\lambda}) \tag{12}$$

$$T_{ij}(\underset{\sim}{\lambda},\underset{\sim}{k}) = \frac{\Omega_{BZ}}{N'}\sum_{q}^{N'}\sum_{g}\alpha_i^*(\underset{\sim}{q}+\underset{\sim}{k}+\underset{\sim}{g})\ \alpha_j(\underset{\sim}{q}+\underset{\sim}{k}+\underset{\sim}{g})\ |\underset{\sim}{k}+\underset{\sim}{g}|^2 \times \exp(-i(\underset{\sim}{q}+\underset{\sim}{k}+\underset{\sim}{g})\cdot\underset{\sim}{\lambda}) \tag{13}$$

$$V_{ij}^{m}(\underset{\sim}{\lambda},\underset{\sim}{k}) = \frac{\Omega_{BZ}}{N'}\sum_{q}^{N'}\sum_{g}\sum_{g'}\alpha_i^*(\underset{\sim}{q}+\underset{\sim}{k}+\underset{\sim}{g}')\ \alpha_j(\underset{\sim}{q}+\underset{\sim}{k}+\underset{\sim}{g})\ V(\underset{\sim}{g}'-\underset{\sim}{g})\ \cos[(\underset{\sim}{g}'-\underset{\sim}{g})\cdot\underset{\sim}{\tau}_m] \times \exp(i(\underset{\sim}{g}'-\underset{\sim}{g})\cdot\tau_m)\ \exp(-i(\underset{\sim}{q}+\underset{\sim}{k}+\underset{\sim}{g})\cdot\underset{\sim}{\lambda}) \tag{14}$$

where the sum $\sum_q^{N'}$ is over N′ wave vectors q across the three dimensional Brillouin zone, along an interval perpendicular (in reciprocal space) to the two dimensional Brillouin zone of the film. In the case of the (111) orientated film the values q range from -(π/a,π/a,π/a) to (π/a,π/a,π/a) and in the case of the (100) film, q ranges from (-2π/a,0,0) to (2π/a,0,0).

Using these expressions for the matrix elements for T,V,U and S and the spin orbit terms within each p orbital matrix sub-block then the two dimensional bandstructure over the sub-bands may be obtained from the matrix equation

$$\sum_{j}^{N}\sum_{\lambda}\{\ H_{j'\lambda',j\lambda}(\underset{\sim}{k}) - E_{nm}(\underset{\sim}{k})\ S_{j'\lambda',j\lambda}(\underset{\sim}{k})\ \} \times C_{mn,j\lambda}(\underset{\sim}{k}) = 0 \tag{15}$$

for the system of N layers and 20 orbitals ϕ_j(r) on each atomic site.

The most important feature not thoroughly treated by this method is the contribution from the reconstruction and relaxation at the surface and the interface with the substrate. The recent work by Continenza and Freeman [2] has started to address the important problem of the bonding between the α-Sn film with a CdTe substrate by studying the

Table 2
The energy levels (eV) of the sub-bands for V_{max} and C_{min} and the energy band gap as a function of the number of layers for (111) and (100) films

Number of Layers	(100) film V_{max}	C_{min}	Gap	(111) film V_{max}	C_{min}	Gap
12	-0.22	0.34	0.56	0.03	0.20	0.17
14	-0.18	0.26	0.44	0.03	0.19	0.16
16	-0.16	0.20	0.36	0.02	0.18	0.16
18	-0.14	0.15	0.29	0.02	0.17	0.15
20	-0.12	0.11	0.23	0.02	0.14	0.12

properties of ultra-thin Sn-CdTe superlattices where only 2 layers of tin occur in the unit cell. The work presented in this paper considers a quantum well with a sufficient number of Sn layers in order to adequately obtain a manifold of sub-bands within the valence bandstructure and the low lying conduction bands.

3 Results

The energy levels for the sub-bands of (111) and (100) oriented α-Sn films have been calculated by the theory outlined in the preceeding section. The behavior of the sub-band structure with film thickness is approached by varying the number of layers from 12 to 20 for each orientation. The energy levels for the valence band maximum V_{max} and the conduction band minimum C_{min} are displayed in table 2 for both the (100) and (111) films.

The relationship between the band gap and thickness for the (111) film is different for the current results than was determined in the earlier study [1] where spin orbit splitting was not included. The current results obtain a significantly smaller band gap for the numbers of layers considered. The bandgap and the change in bandgap with film thickness is considerably larger for the (100) film than the (111) film. These values have been obtained for an assumed value for U_0 of 1.5eV.

The dependence of the bandgap on the interface parameter U_0 is displayed in table 3 for 12 layer films. Increasing the parameter U_0 leads to an increase in the bandgap for a (100) film but a decrease for the (111) film. This sign of the bandgap change follows from the relative difference between the positive changes in both V_{max} and C_{min}. The value of U_0 describes the potential barrier for electrons within the α-Sn film induced by the adjoining material or surface. These results show that the band gap for thin α-Sn films might vary significantly with different materials at the film barriers.

Table 3
The band gap for a range of values of U_0

Film	U_0 (eV)	V_{max}	C_{min}	Gap (eV)
(111)	0	-0.065	0.190	0.255
(111)	1.5	0.030	0.203	0.173
(111)	2.5	0.099	0.205	0.106
(100)	1.5	-0.216	0.337	0.553
(100)	2.5	-0.144	0.551	0.695

The altering and tuning of the α-Sn bandstructure is of considerable interest. Large optical nonlinearities have recently been reported [20] and α-Sn based structures may have application at infra-red and microwave frequencies. Recent experiments [6,20] closely examine the L-Γ energy gap of α-Sn films. A detailed study of the two dimensional electronic structure derived from the bulk Γ and L levels is therefore important.

In the case of the (111) orientated film the bulk symmetry points Γ (0,0,0), L (1/2,1/2,1/2) and L (-1/2,-1/2,-1/2) all project to the Γ point of film. The six other L point wave vectors project to symmetry points on the Brillouin zone edge. The low lying conduction levels of these six points for the 16 layer (111) film are 0.238 eV greater than the conduction band minimum at Γ. In the case of the (100) film the 8 bulk L point project to the film Brillouin zone edge. The conduction levels are only 0.072 eV above the conduction band minimum at the Γ point. The smaller difference for the (100) film result from the higher value for the conduction band minimum for the (100) film as compared to (111) film.

The valence sub-bands near V_{max} for the (111) film describe the thin film induced quantisation of the highest (fourth) valence band for wave vectors in the (111) direction (Γ to L). The bulk dispersion is shown in figure 1. This bulk band disperses to lower energy from Γ to L at a rate approximately 50% faster than that suggested by the sub-band energy levels m=1 to 4 obtained for the various films. The narrower range of energies found for such sub-band levels is partly due to the interaction with the low lying conduction band occurring closely above the fourth valence band in the Γ to L dispersion. This interaction results from the strong perturbation U(r) and is compounded by the spin orbit interaction between the p orbitals.

The occupation of the sub-bands near the narrow band gap may be strongly influenced by the type of doping within the substrate. The substrate may also influence the position of the interface localised resonances with respect to the band gap and the Fermi energy. Recent experiments have observed some resonance behavior at the interface of α-Sn films with InSb and variations in the results with substrate doping [9].

4 Conclusions

A tight binding method has been developed to describe the electronic structure of a zero band gap semiconductor. The spin orbit interaction and the dispersions of the bands are included into the calculation of the electronic structure of α-Sn. The general behaviour of the quantum well induced sub-band electronic structure has been adequately described by an extension of this method. In order to develop this approach further to examine the band gap engineering of α-Sn and other zero and narrow band gap semiconductors, the important influence played by the film boundaries needs to be considered.

References:

[1] B.I.Craig and B.J.Garrison, Phys.Rev.B **33** 8130 (1986)

[2] A.Continenza and A.J.Freeman, Phys.Rev.B **43** 8951 (1991)

[3] S.Takatani and Y.W.Chung, Phys.Rev.B **31** 2290 (1985)

[4] H.Hochst, D.W.Niles and I.Hernandez-Calderon, J.Vac.Sci.Technol. B **6** 1219 (1988)

[5] M.Tang, D.W.Niles, I.Hernandez-Calderon and H.Hochst, Phys.Rev.B **36** 3336 (1987)

[6] C.A.Hoffman, J.R.Meyer, R.J.Wagner, F.J.Bartoli, M.A.Engelhardt and H.Hochst, Phys.Rev.B **40** 11693 (1989)

[7] L.W.Tu, G.K.Wong, S.N.Song, Z.Zhao and J.B.Ketterson, Appl.Phys.Lett. **55** 2643 (1989)

[8] S.N.Song, X.J.Yi, J.Q.Zheng, Z.Zhao, L.W.Tu, G.K.Wong and J.B.Ketterson, Appl.Phys.Lett.**56** 227 (1990)

[9] W.T.Yuen, W.K.Liu, R.A.Stradling and B.A.Joyce, J.Crystal Growth **111** 943 (1991)

[10] D.J.Chadi Phys.Rev.B **16** 3572 (1977)

[11] M.Downey and P.V.Smith, phys.stat.solidi B **115** 255 (1983)

[12] P.V.Smith phys.stat.solidi B **116** 101 (1983)

[13] D.J.Chadi Phys.Rev.B **16** 790 (1977)

[14] K.C.Hass, H.Ehrenreich and B.Velicky Phys.Rev.B **27** 1088 (1983)

[15] M.L.Cohen and T.K.Bergstresser, Phys.Rev.**141** 789 (1966)

[16] J.R.Chelikowsky and M.L.Cohen, Phys.Rev.B **14** 556 (1976)

[17] A-B.Chen and A.Sher, J.Vac.Sci.Technol. **21** 138 (1982)

[18] R.D.Graft, J.Vac.Sci.Technol. **21** 146 (1982)

[19] P.Vogl,H.P.Hjalmarson and J.D.Dow J.Phys.Chem.Solids **44** 365 (1983)

[20] E.R.Youngdale,C.A.Hoffman,J.R.Meyer F.J.Bartoli, M.A.Engelhardt and H.Hochst Semicond.Sci.Technol. **5** S253 (1990)